

Investigating the Properties of Aqueous Monoisopropanolamine Using Density Data from 283.15 K to 353.15 K

Y. Leong Yeow · Jian Ge · Yee-Kwong Leong · Ash Khan

Received: 4 January 2008 / Accepted: 31 December 2008 / Published online: 21 January 2009
© Springer Science+Business Media, LLC 2009

Abstract The published isothermal density data of aqueous monoisopropanolamine (MIPA) for different temperatures are converted into molar volumes as a function of composition. Tikhonov regularization is applied to obtain the derivatives of molar volume with respect to composition. These derivatives are used to compute the two partial molar volumes of the aqueous solution covering the entire composition range and for all the temperatures reported. A second application of Tikhonov regularization is then used to obtain the partial molar coefficients of the thermal expansion of the solution under constant pressure. This is followed by an examination of the second derivative of the partial molar volumes with respect to temperature over the entire composition range. The signs of these derivatives, for different compositions and temperatures, allow the change in the molecular interaction between MIPA and water in aqueous solution to be discussed.

Keywords Aqueous monoisopropanolamine · Partial molar volumes · Thermal expansion · Coefficient · Tikhonov regularization

Y. Leong Yeow (✉) · J. Ge
Department of Chemical and Biomolecular Engineering,
The University of Melbourne,
Parkville, VIC 3010, Australia
e-mail: yly@unimelb.edu.au

Y.-K. Leong
School of Mechanical Engineering,
The University of Western Australia,
Crawley, WA 6009, Australia

A. Khan
CO₂ Cooperative Research Centre,
Parkville, VIC 3010, Australia

1 Introduction

Aqueous monoisopropanolamine (MIPA) is one of the several alkanolamine solutions used in the absorption of carbon dioxide, sulfur dioxide, and hydrogen sulfide gases in the process industry. As an absorption agent, MIPA is less widely used than, for example, monoethanolamine or diethanolamine, but it is said to have the advantage of a higher reaction rate with some of these gases when compared to the more common alkanolamines [1]. A quick examination of the patent literature reveals that MIPA is the starting material in many laboratory and industrial organic synthesis processes. It is also an important constituent, serving variously as a stabilizer, emulsifier, and pH control agent, in the formulation of a large number of industrial, household, pharmaceutical, and cosmetic products. Apart from their practical importance, the thermodynamic and transport properties of the MIPA–water system are also of fundamental interest to physical chemists and consequently these have been reported by a number of investigators [2–6].

The aim of this research is to apply the recently reported Tikhonov regularization technique [7,8] in order to convert the density data of aqueous MIPA reported by Mokraoui et al. [4] into partial molar volumes \bar{V}_{MIPA} and \bar{V}_{W} of MIPA and water, respectively. This new technique allows the partial molar volumes to be obtained more easily and more reliably. The data in [4] include not only the density at closely spaced compositions, but also the density at a series of regularly spaced temperatures T . Through a second application of Tikhonov regularization, the non-isothermal partial molar volumes at fixed compositions are converted into isobaric coefficients of thermal expansion of aqueous MIPA over the entire composition range and for the range of temperatures reported in [4]. Variations of the partial molar volumes with temperature and composition are then examined with the objective of detecting the change, if any, in the interaction between MIPA and water molecules in the aqueous solution.

2 Molar Volume Data and Numerical Method

Mokraoui et al. [4] measured the mass density $\rho(x_{\text{W}})$ of aqueous MIPA solutions, at atmospheric pressure, for $283.15 \text{ K} \leq T \leq 353.15 \text{ K}$ [4]. For each T , they tabulated the density at 21 different mole fractions of water between the range of $0.0438 \leq x_{\text{W}} \leq 0.9600$. These data are converted into molar volume by using the following simple expression,

$$v(x_{\text{W}}) = \frac{x_{\text{W}}M_{\text{W}} + (1 - x_{\text{W}})M_{\text{MIPA}}}{\rho(x_{\text{W}})}, \quad (1)$$

where M_{MIPA} and M_{W} are the molar masses of MIPA and water, respectively. As $v(x_{\text{W}})$ can be computed directly from the tabulated $\rho(x_{\text{W}})$ data in [4], they will not be presented here. For each temperature, the resulting $v(x_{\text{W}})$ data are extended to include that of pure MIPA and pure water. The densities of the pure components at different temperatures are taken from [4] for MIPA and [9] for water.

The partial molar volumes \bar{V}_{MIPA} and \bar{V}_{W} are related to $v(x_{\text{W}})$ by [10]

$$\bar{V}_{\text{MIPA}} = v - x_{\text{W}} \frac{\partial v}{\partial x_{\text{W}}}, \quad \bar{V}_{\text{W}} = v + x_{\text{MIPA}} \frac{\partial v}{\partial x_{\text{W}}} \quad (2)$$

with the understanding that the temperature and pressure are held fixed in these partial derivatives. For simplicity, subscripts normally used to indicate the thermodynamic variables that are being held fixed have been omitted here and in most of the subsequent derivatives. The critical step in applying Eq. 2 to obtain the partial molar volumes is the differentiation of the experimental $v(x_{\text{W}})$ data. If this is not carefully performed, the differentiation operation will amplify the measurement noise in $v(x_{\text{W}})$, leading to a noisy derivative and consequently unreliable partial molar volumes [7]. The usual practice is to fit low-order polynomials to the experimental data and compute the required derivatives by differentiating the fitted curves. It is well known that two different fitted curves that describe the same set of $v(x_{\text{W}})$ data to the same degree of accuracy do not necessarily have derivatives that are in agreement with one another. This is because differentiation is likely to amplify the local and usually minor differences between two nearly identical fitted curves [7]. The Tikhonov regularization procedure used to compute the partial derivative $\partial v / \partial x_{\text{W}}$ in this research has a built-in regularization parameter λ that is able to keep the noise amplification under control [7]. The mathematical principles of the Tikhonov regularization procedure can be found in [7, 8]. Some of its advantages over existing curve fitting methods, when applied to evaluate isothermal partial molar volumes of a number of different binary solutions, are discussed in [8, 11, 12]. Apart from the short description in the following paragraph to introduce the key equations of Tikhonov regularization, detailed development of this procedure and its implementation on computers will be omitted. Interested readers are directed particularly to [8].

For the purpose of introducing Tikhonov regularization, it is convenient to denote the first and second derivatives of $v(x_{\text{W}})$ by $r(x_{\text{W}}) = \partial v / \partial x_{\text{W}}$ and $f(x_{\text{W}}) = \partial^2 v / \partial x_{\text{W}}^2$. In terms of these derivatives, $v(x_{\text{W}})$ is given by [13]

$$v^{\text{C}}(x_{\text{W}}) = \int_{x'=0}^{x_{\text{W}}} (x_{\text{W}} - x') f(x') dx' + v_0 + x_{\text{W}} r_0. \quad (3)$$

Superscript C is used to distinguish the computed molar volume from its experimentally measured counterpart, which will be denoted by $v^{\text{M}}(x_{\text{W}})$. Equation 3 is exact and is based on a two-term Taylor's series expansion of $v(x_{\text{W}})$ about $x_{\text{W}} = 0$. The integral on the right-hand side of Eq. 3 is the remainder term of the Taylor's series in integral form [13]. Tikhonov regularization solves this equation for the unknown second derivative $f(x_{\text{W}})$ together with the unknown constants $r(0) = r_0$ and $v(0) = v_0$, i.e., the value of the first derivative and that of the molar volume of pure water. This is achieved by finding the discretized $f(x_{\text{W}})$ and the constants r_0 and v_0 that minimize the sum of the squares of the differences between the experimental data $v^{\text{M}}(x_{\text{W}})$ and the back-calculated $v^{\text{C}}(x_{\text{W}})$. In processing the $v(x_{\text{W}})$ data sets from [4], the choice of the regularization parameter λ is guided by general cross validation (GCV) [14]. An appropriate λ will ensure that the resulting $f(x_{\text{W}})$ does not show excessive and physically unreal fluctuations.

3 Results and Discussion

3.1 Partial Molar Volumes

For each set of the $v(x_W)$ data, the discretized $f(x_W)$ given by Tikhonov regularization is integrated to yield the first derivative $r(x_W)$ needed in Eq. 2. For checking purposes, this first derivative is further integrated to give the back-calculated specific volume $v^C(x_W)$, and this is compared against the corresponding experimental specific volume data $v^M(x_W)$. Since numerical integration is a well-behaved operation that does not amplify noise, these two integration steps were carried out using standard commercial software. For all the cases investigated, the average difference between $v^M(x_W)$ and $v^C(x_W)$ is less than a tiny fraction of 1%, thereby confirming the reliability of the derivatives generated by Tikhonov regularization.

The partial molar volumes \bar{V}_W and that of \bar{V}_{MIPA} obtained by substituting $r(x_W) = \partial v / \partial x_W$ and $v^C(x_W)$ into Eq. 2 are tabulated in Table 1. They cover the entire composition range $0 \leq x_W \leq 1$ and all the temperatures investigated by Mokraoui et al. [4]. These partial molar volumes have been compared against that obtained by using the least-squares fitted parameters reported in [4], and they are found to be in very satisfactory agreement. Compared to the least-squares procedure reported in [4], the Tikhonov regularization procedure is computationally simpler even though the mathematical analysis behind it may appear to be more complex.

To examine the overall behaviors of \bar{V}_W and \bar{V}_{MIPA} generated by Tikhonov regularization, they are shown graphically in Fig. 1a and b. In these plots, the temperature varied from $T = 283.15$ K for the bottommost curve to $T = 353.15$ K for the topmost curve. The temperatures for the in-between curves are as listed in Table 1. The most prominent features of the partial molar volume curves are the large minima exhibited by all the \bar{V}_{MIPA} curves in the neighborhood of $x_W = 0.9$ (Fig. 1a). As required by the Gibbs–Duhem relationship between the partial molar volumes of binary solutions, at each of these minima of the \bar{V}_{MIPA} curves, the \bar{V}_W curves exhibit a maximum. These maxima are much smaller in size, and consequently some of them do not show up clearly in the curves in Fig. 1b. However, they can be observed in enlarged localized plots.

The partial molar volume plots in Fig. 1 show that, for any x_W , both \bar{V}_{MIPA} and \bar{V}_W increase with T . At some isolated x_W , the partial molar volume curves can become closely bunched up, but they do not appear to intersect one another. In particular, both of the partial molar volumes at infinite dilution, i.e., \bar{V}_{MIPA} at $x_W = 1$ and \bar{V}_W at $x_W = 0$, increase with T . These are in a satisfactory agreement with the recent corrected partial molar volumes at infinite dilution reported by Mokraoui et al. [5].

3.2 Coefficients of Thermal Expansion

An important material property of solutions undergoing constant pressure heating is the isobaric coefficient of thermal expansion defined by $\alpha = (1/v)\partial v/\partial T$. For a binary solution such as aqueous MIPA, starting from the expression $v = x_W\bar{V}_W + (1 - x_W)\bar{V}_{MIPA}$, α can be expressed in terms of partial molar quantities,

Table 1 Partial molar volumes for $T = 283.15$ K to $T = 353.15$ K; \bar{V}_{MIPA} and \bar{V}_{W} are in $\text{cm}^3 \cdot \text{mol}^{-1}$

T (K)	283.15		288.15		293.15		298.15		303.15	
	\bar{V}_{MIPA}	\bar{V}_{W}	\bar{V}_{MIPA}	\bar{V}_{W}	\bar{V}_{MIPA}	\bar{V}_{W}	\bar{V}_{MIPA}	\bar{V}_{W}	\bar{V}_{MIPA}	\bar{V}_{W}
0	77.5707	15.1372	77.8868	15.1613	78.2079	15.1479	78.5334	15.1758	78.8641	15.1800
0.05	77.5665	15.3125	77.8828	15.3230	78.2031	15.3467	78.5287	15.3666	78.8588	15.3925
0.1	77.5558	15.4446	77.8715	15.4623	78.1913	15.4927	78.5164	15.5191	78.8462	15.5507
0.15	77.5389	15.5644	77.8531	15.5923	78.1740	15.6153	78.4986	15.6452	78.8289	15.6730
0.2	77.5288	15.6141	77.8428	15.6434	78.1625	15.6714	78.4867	15.7033	78.8163	15.7341
0.25	77.5194	15.6451	77.8332	15.6751	78.1496	15.7147	78.4719	15.7529	78.7988	15.7930
0.3	77.4733	15.7644	77.7836	15.8033	78.0990	15.8457	78.4192	15.8896	78.7440	15.9352
0.35	77.3807	15.9561	77.6871	16.0031	78.0036	16.0432	78.3228	16.0894	78.6475	16.1351
0.4	77.2895	16.1092	77.5955	16.1572	77.9086	16.2025	78.2257	16.2521	78.5488	16.3006
0.45	77.2109	16.2154	77.5183	16.2615	77.8246	16.3162	78.1388	16.3697	78.4569	16.4248
0.5	77.0838	16.3548	77.3902	16.4019	77.6946	16.4588	78.0072	16.5141	78.3219	16.5731
0.55	76.8897	16.5298	77.1900	16.5824	77.4951	16.6386	77.8052	16.6961	78.1192	16.7557
0.6	76.6272	16.7230	76.9200	16.7812	77.2247	16.8377	77.5337	16.8961	77.8488	16.9550
0.65	76.2614	16.9416	76.5563	16.9986	76.8645	17.0531	77.1782	17.1088	77.4973	17.1653
0.7	75.7633	17.1803	76.0744	17.2296	76.3924	17.2795	76.7168	17.3300	77.0447	17.3824
0.75	75.0554	17.4471	75.3965	17.4852	75.7380	17.5263	76.0846	17.5685	76.4336	17.6130
0.8	74.0577	17.7352	74.4495	17.7587	74.8406	17.7856	75.2309	17.8153	75.6221	17.8476
0.85	72.8939	17.9826	73.3586	17.9907	73.8198	18.0027	74.2719	18.0193	74.7193	18.0397
0.9	72.1200	18.0978	72.6333	18.0985	73.1354	18.1043	73.6218	18.1157	74.0975	18.1317
0.95	72.5517	18.0703	73.0000	18.0756	73.4315	18.0864	73.8516	18.1025	74.2622	18.1232
1	74.7742	18.0214	74.9729	18.0322	75.1599	18.0485	75.3609	18.0695	75.5658	18.0949

Table 1 continued

T (K)	308.15		313.15		318.15		323.15		328.15	
	\bar{V}_{MIPA}	\bar{V}_W	\bar{V}_{MIPA}	\bar{V}_W	\bar{V}_{MIPA}	\bar{V}_W	\bar{V}_{MIPA}	\bar{V}_W	\bar{V}_{MIPA}	\bar{V}_W
0	79.1993	15.2351	79.5398	15.2599	79.8867	15.2618	80.2383	15.2889	80.5956	15.3381
0.05	79.1947	15.4177	79.5350	15.4512	79.8813	15.4786	80.2327	15.5116	80.5902	15.5550
0.1	79.1819	15.5764	79.5220	15.6130	79.8677	15.6498	80.2186	15.6874	80.5765	15.7267
0.15	79.1631	15.7099	79.5035	15.7438	79.8494	15.7795	80.2000	15.8194	80.5583	15.8557
0.2	79.1496	15.7752	79.4894	15.8119	79.8346	15.8505	80.1842	15.8951	80.5413	15.9364
0.25	79.1323	15.8332	79.4700	15.8775	79.8126	15.9248	80.1605	15.9754	80.5147	16.0268
0.3	79.0769	15.9770	79.4128	16.0259	79.7535	16.0786	80.1005	16.1316	80.4529	16.1879
0.35	78.9777	16.1827	79.3128	16.2331	79.6534	16.2860	80.0008	16.3383	80.3532	16.3946
0.4	78.8750	16.3548	79.2085	16.4079	79.5477	16.4629	79.8932	16.5182	80.2438	16.5774
0.45	78.7803	16.4828	79.1110	16.5398	79.4463	16.6001	79.7869	16.6621	80.1336	16.7265
0.5	78.6449	16.6315	78.9729	16.6915	79.3058	16.7545	79.6433	16.8199	79.9885	16.8862
0.55	78.4416	16.8148	78.7675	16.8766	79.1005	16.9396	79.4386	17.0046	79.7841	17.0705
0.6	78.1700	17.0148	78.4960	17.0767	78.8303	17.1388	79.1712	17.2017	79.5174	17.2670
0.65	77.8209	17.2237	78.1515	17.2829	78.4894	17.3428	78.8344	17.4032	79.1841	17.4666
0.7	77.3775	17.4365	77.7178	17.4910	78.0634	17.5473	78.4143	17.6049	78.7718	17.6645
0.75	76.7883	17.6589	77.1467	17.7067	77.5096	17.7565	77.8742	17.8089	78.2474	17.8627
0.8	76.0169	17.8820	76.4079	17.9204	76.8028	17.9610	77.1968	18.0051	77.5967	18.0511
0.85	75.1615	18.0640	75.5977	18.0928	76.0324	18.1249	76.4654	18.1607	76.8983	18.1998
0.9	74.5581	18.1531	75.0179	18.1782	75.4693	18.2077	75.9197	18.2407	76.3665	18.2776
0.95	74.6655	18.1488	75.0693	18.1779	75.4679	18.2113	75.8687	18.2479	76.2689	18.2882
1	75.8034	18.1243	76.0291	18.1574	76.2718	18.1943	76.5238	18.2343	76.7861	18.2777

Table 1 continued

T (K)	333.15		338.15		343.15		348.15		353.15	
	\bar{V}_{MIPA}	\bar{V}_W	\bar{V}_{MIPA}	\bar{V}_W	\bar{V}_{MIPA}	\bar{V}_W	\bar{V}_{MIPA}	\bar{V}_W	\bar{V}_{MIPA}	\bar{V}_W
0	80.9589	15.3919	81.3307	15.4081	81.7083	15.4421	82.0933	15.4960	82.4870	15.5456
0.05	80.9537	15.5986	81.3251	15.6324	81.7024	15.6811	82.0876	15.7252	82.4814	15.7731
0.1	80.9400	15.7697	81.3107	15.8118	81.6879	15.8629	82.0731	15.9061	82.4671	15.9512
0.15	80.9212	15.9031	81.2917	15.9465	81.6692	15.9951	82.0535	16.0442	82.4476	16.0891
0.2	80.9031	15.9889	81.2727	16.0368	81.6492	16.0900	82.0310	16.1508	82.4231	16.2045
0.25	80.8756	16.0823	81.2427	16.1386	81.6170	16.1997	81.9963	16.2693	82.3850	16.3345
0.3	80.8135	16.2444	81.1789	16.3051	81.5526	16.3678	81.9324	16.4362	82.3199	16.5052
0.35	80.7134	16.4518	81.0788	16.5127	81.4534	16.5734	81.8359	16.6362	82.2243	16.7031
0.4	80.6021	16.6378	80.9661	16.7009	81.3394	16.7638	81.7213	16.8274	82.1089	16.8956
0.45	80.4886	16.7913	80.8492	16.8590	81.2181	16.9278	81.5952	16.9979	81.9788	17.0715
0.5	80.3417	16.9530	80.7004	17.0229	81.0669	17.0944	81.4408	17.1681	81.8218	17.2447
0.55	80.1371	17.1375	80.4965	17.2067	80.8643	17.2771	81.2395	17.3498	81.6221	17.4250
0.6	79.8712	17.3335	80.2328	17.4012	80.6035	17.4694	80.9820	17.5396	81.3688	17.6117
0.65	79.5410	17.5312	79.9060	17.5969	80.2798	17.6632	80.6618	17.7313	81.0527	17.8009
0.7	79.1353	17.7260	79.5062	17.7889	79.8838	17.8534	80.2695	17.9197	80.6637	17.9877
0.75	78.6248	17.9190	79.0081	17.9772	79.3956	18.0381	79.7907	18.1009	80.1931	18.1658
0.8	77.9997	18.1001	78.4062	18.1516	78.8151	18.2063	79.2307	18.2633	79.6525	18.3227
0.85	77.3330	18.2419	77.7677	18.2875	78.2053	18.3361	78.6473	18.3874	79.0952	18.4413
0.9	76.8127	18.3179	77.2573	18.3618	77.7070	18.4085	78.1583	18.4583	78.6148	18.5107
0.95	76.6706	18.3318	77.0747	18.3787	77.4835	18.4283	77.8945	18.4811	78.3088	18.5367
1	77.0626	18.3242	77.3537	18.3736	77.6420	18.4261	77.9409	18.4814	78.2393	18.5396

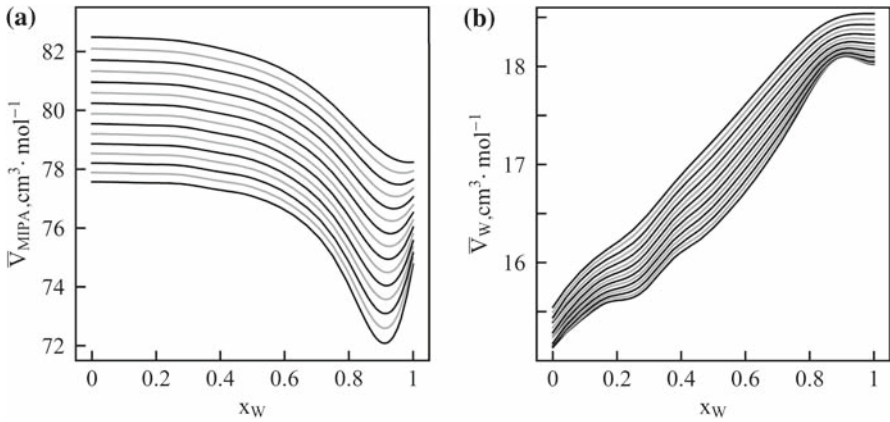


Fig. 1 Partial molar volumes of MIPA and water for temperatures between 283.15 K (*bottommost curve*) and 353.15 K (*topmost*) at 5 K intervals: (a) MIPA and (b) water

$$\begin{aligned}
 \alpha &= \frac{1}{v} \frac{\partial [x_w \bar{V}_w + (1 - x_w) \bar{V}_{MIPA}]}{\partial T} \\
 &= \frac{x_w \bar{V}_w}{v} \frac{1}{\bar{V}_w} \frac{\partial \bar{V}_w}{\partial T} + \frac{(1 - x_w) \bar{V}_{MIPA}}{v} \frac{1}{\bar{V}_{MIPA}} \frac{\partial \bar{V}_{MIPA}}{\partial T} \\
 &= \bar{\phi}_w \bar{\alpha}_w + \bar{\phi}_{MIPA} \bar{\alpha}_{MIPA},
 \end{aligned}
 \tag{4}$$

where

$$\bar{\phi}_{MIPA} = \frac{(1 - x_w) \bar{V}_{MIPA}}{v}, \quad \bar{\phi}_w = \frac{x_w \bar{V}_w}{v}
 \tag{5}$$

and

$$\bar{\alpha}_{MIPA} = \frac{1}{\bar{V}_{MIPA}} \frac{\partial \bar{V}_{MIPA}}{\partial T}, \quad \bar{\alpha}_w = \frac{1}{\bar{V}_w} \frac{\partial \bar{V}_w}{\partial T}.
 \tag{6}$$

Equation 5 can be regarded as the definition of partial molar volume fractions and Eq. 6 as the definition of partial molar coefficients of thermal expansion.

In evaluating the partial derivatives in Eq. 6, it is understood that both pressure P and x_w are held fixed. This is achieved by treating the computed \bar{V}_{MIPA} and \bar{V}_w in Table 1 as functions of T with composition x_w held at a fixed value. Examples of constant composition plots are shown in Fig. 2a and b for \bar{V}_{MIPA} and Fig. 2c for \bar{V}_w . For clarity, the constant composition data for \bar{V}_{MIPA} are shown in two separate plots. In order that the \bar{V}_{MIPA} data for $x_w = 0$, i.e., for pure MIPA, can be clearly observed, these are shown in Fig. 2b instead of Fig. 2a. Based on the data available, there are only 15 points on each of the constant composition curves and these points are at a comparatively large temperature interval of 5 K. It is essential to allow for this paucity of data when considering all the subsequent results.

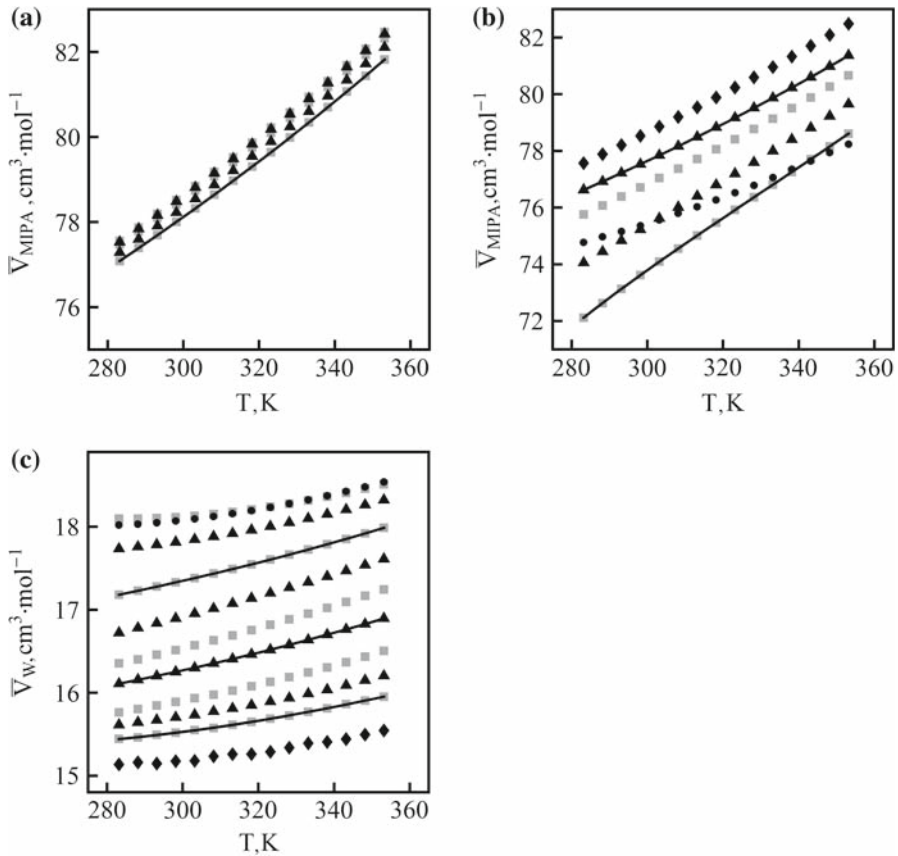


Fig. 2 Variation of partial molar volumes with temperature at constant composition. Discrete points in (a) and (b) are for MIPA and those in (c) are for water. \blacksquare : $x_W = 0.1, 0.3, 0.5, 0.7, 0.9$; \blacktriangle : $x_W = 0.2, 0.4, 0.6, 0.8$; \blacklozenge : $x_W = 0.0$; and \bullet : $x_W = 1.0$. Continuous curve in (a) is the back-calculated $\bar{V}_{\text{MIPA}}^{\text{C}}(T)$ for $x_W = 0.5$; those in (b) are for $x_W = 0.6$ (upper curve) and 0.9 (lower curve). Continuous curves in (c) are $\bar{V}_W^{\text{C}}(T)$ for $x_W = 0.1$ (lower curve), 0.4 (middle curve), and 0.7 (upper curve)

Tikhonov regularization is now applied to evaluate the second derivatives $\partial^2 \bar{V}_{\text{MIPA}} / \partial T^2$ and $\partial^2 \bar{V}_W / \partial T^2$ of the constant x_W data. The basic steps are the same as in the evaluation of $\partial^2 v / \partial x_W^2$. Because of the smaller number of points in each of the constant x_W data sets, the regularization parameter λ is now guided by the Morozov principle instead of GCV [7]. As before, the second derivatives are integrated once to yield $\partial \bar{V}_{\text{MIPA}} / \partial T$ and $\partial \bar{V}_W / \partial T$ and then integrated a second time to give the back-calculated $\bar{V}_{\text{MIPA}}^{\text{C}}(T)$ and $\bar{V}_W^{\text{C}}(T)$. The reliability of the derivatives with respect to T are, again as before, checked by comparing the back-calculated partial molar volumes with the discrete points in Fig. 2. Typical examples of the back-calculated $\bar{V}_{\text{MIPA}}^{\text{C}}(T)$ and $\bar{V}_W^{\text{C}}(T)$ are shown as continuous curves in Fig. 2. In general, the average difference

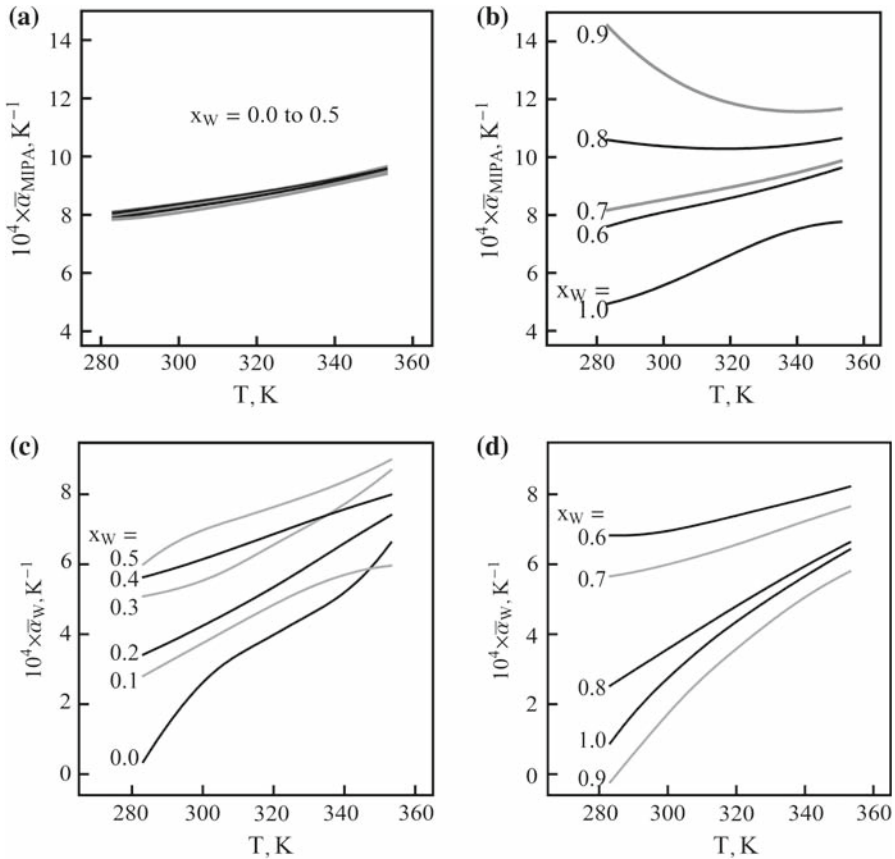


Fig. 3 Partial molar coefficients of thermal expansion as a function of temperature. Composition is indicated by the figure next to each of the curves: (a), (b) MIPA and (c), (d) water

between the discrete points and the continuous $\bar{V}_W^C(T)$ and $\bar{V}_{MIPA}^C(T)$ curves is again less than a small fraction of 1%.

The $\bar{\alpha}_{MIPA}$ and $\bar{\alpha}_W$ obtained by substituting $\partial\bar{V}_{MIPA}/\partial T$ and $\partial\bar{V}_W/\partial T$ together with $\bar{V}_{MIPA}^C(T)$ and $\bar{V}_W^C(T)$ into Eq. 6 are tabulated in Tables 2 and 3 and plotted in Fig. 3.

Figure 3a shows that, for $0 \leq x_W \leq 0.5$, all the $\bar{\alpha}_{MIPA}$ curves are closely bunched up. The accuracy of the numerical results is unable to resolve them reliably. But it is clear that all these $\bar{\alpha}_{MIPA}$ increase slightly with increasing T . Figure 3b shows that, for $x_W \geq 0.6$, the $\bar{\alpha}_{MIPA}$ curves begin to spread out and increase significantly as x_W becomes larger, attaining a maximum at $x_W \approx 0.9$. Beyond that, the $\bar{\alpha}_{MIPA}$ curve drops significantly. This change in trend is clearly tied with extrema in the partial molar volumes in the neighborhood of $x_W = 0.9$. As shown in Fig. 3a, all the $\bar{\alpha}_{MIPA}$ shown in Fig. 3b also increase with T except in the neighborhood of $x_W = 0.9$, where they decrease with T .

Table 2 Partial molar coefficients of thermal expansion of MIPA

x_w	0	0.1	0.2	0.3	0.4	0.5	0.6	0.7	0.8	0.9	1.0	
T (K)	$10^4 \times \bar{\alpha}_{MIPA} \text{ (K}^{-1}\text{)}$											
288.15	8.18125	8.16140	8.14507	8.04647	7.98493	7.89128	7.77351	8.28124	10.5197	13.9691	5.09060	
293.15	8.26628	8.25094	8.23299	8.14274	8.07767	7.95751	7.92147	8.38774	10.4526	13.4691	5.27560	
298.15	8.35375	8.34205	8.32274	8.23891	8.17346	8.04346	8.05411	8.49308	10.3969	13.0368	5.48934	
303.15	8.44380	8.43468	8.41453	8.33524	8.27256	8.14309	8.17657	8.59793	10.3525	12.6705	5.72730	
308.15	8.53674	8.52912	8.50881	8.43236	8.37543	8.24949	8.29538	8.70331	10.3198	12.3676	5.98294	
313.15	8.63314	8.62617	8.60622	8.53148	8.48272	8.35856	8.41603	8.81031	10.2993	12.1236	6.24943	
318.15	8.73387	8.72714	8.70749	8.63420	8.59513	8.47100	8.54168	8.92007	10.2922	11.9321	6.51988	
323.15	8.84007	8.83349	8.81345	8.74196	8.71348	8.59002	8.67388	9.03394	10.2991	11.7865	6.78608	
328.15	8.95293	8.94655	8.92486	8.85565	8.83857	8.71730	8.81391	9.15339	10.3206	11.6813	7.03780	
333.15	9.07341	9.06756	9.04235	8.97555	8.97102	8.85150	8.96262	9.27978	10.3571	11.6130	7.26388	
338.15	9.20198	9.19764	9.16637	9.10149	9.11113	8.98991	9.11971	9.41420	10.4085	11.5794	7.45449	
343.15	9.33883	9.33770	9.29718	9.23317	9.25885	9.13019	9.28389	9.55726	10.4747	11.5794	7.60334	
348.15	9.48396	9.48817	9.43486	9.37030	9.41396	9.27096	9.45389	9.70920	10.5557	11.6122	7.70776	
353.15	9.63724	9.64904	9.57936	9.51271	9.57624	9.41170	9.6291	9.86989	10.6511	11.6769	7.76744	

Table 3 Partial molar coefficients of thermal expansion of water

x_W	0	0.1	0.2	0.3	0.4	0.5	0.6	0.7	0.8	0.9	1.0	
T (K)	$10^4 \times \bar{\alpha}_W$ (K ⁻¹)											
283.15	0.35628	2.80976	3.41921	5.08740	5.63181	5.99615	6.82766	5.65885	2.52850	-0.2305	0.88264	
288.15	1.12940	3.08966	3.65427	5.18792	5.77240	6.36889	6.82943	5.74106	2.84377	0.36424	1.51505	
293.15	1.82471	3.36876	3.89851	5.31429	5.92439	6.66902	6.86313	5.84000	3.15639	0.95109	2.07606	
298.15	2.42844	3.64732	4.15134	5.47035	6.08684	6.90453	6.92618	5.95399	3.46684	1.52253	2.57442	
303.15	2.92052	3.92588	4.41172	5.66451	6.25772	7.09313	7.01309	6.07936	3.77618	2.06411	3.02869	
308.15	3.29936	4.20428	4.67914	5.90184	6.43445	7.25753	7.11668	6.21280	4.08507	2.56213	3.45631	
313.15	3.60134	4.48054	4.95482	6.17291	6.61485	7.41640	7.23024	6.35422	4.39243	3.01537	3.85920	
318.15	3.88152	4.75052	5.24133	6.45659	6.79745	7.57838	7.34923	6.50547	4.69590	3.43587	4.23079	
323.15	4.16703	5.00841	5.54028	6.73666	6.98067	7.74474	7.47079	6.66665	4.99342	3.83732	4.57838	
328.15	4.45134	5.24739	5.85064	7.01260	7.16220	7.91635	7.59251	6.83449	5.28428	4.22530	4.91323	
333.15	4.73647	5.46053	6.16838	7.29658	7.33951	8.09707	7.71317	7.00404	5.56867	4.59507	5.23629	
338.15	5.05935	5.64180	6.48785	7.60257	7.51099	8.29216	7.83416	7.17149	5.84652	4.93884	5.54756	
343.15	5.46753	5.78704	6.80354	7.93799	7.67648	8.50579	7.95873	7.33516	6.11712	5.25376	5.84950	
348.15	5.98750	5.89431	7.11146	8.30356	7.83657	8.74012	8.08955	7.49466	6.37970	5.54077	6.14340	
353.15	6.62513	5.96336	7.40991	8.69788	7.99169	8.99557	8.22760	7.64994	6.63396	5.80041	6.42892	

Figure 3c,d shows that the partial molar coefficient of the thermal expansion for water exhibits a different trend. For $0 \leq x_W \leq 0.6$ (approx.), the $\bar{\alpha}_W$ curves move toward higher and higher values as x_W is increased. Beyond $x_W = 0.6$, this increasing trend is reversed and the $\bar{\alpha}_W$ curve attains a minimum at $x_W \approx 0.9$. Finally, for $x_W = 1.0$, i.e., pure water, $\bar{\alpha}_W$ moved above that for $x_W = 0.9$ indicating the re-emergence of the increasing trend. It is noticed that $\bar{\alpha}_W$ increases with T for all x_W , but the rate of increase is significantly non-uniform.

To ensure that the behaviors exhibited by the computed $\bar{\alpha}_{\text{MIPA}}$ and $\bar{\alpha}_W$ are not numerical artifacts, a simple check has been carried out. By definition, when $x_W = 0$, $\bar{\alpha}_{\text{MIPA}} \equiv \alpha_{\text{MIPA}}$ and when $x_W = 1$, $\bar{\alpha}_W \equiv \alpha_W$, i.e., they become the normal coefficients of thermal expansion of pure MIPA and water, respectively. Mokraoui et al. [4] reported extensive density versus temperature data of pure MIPA. Based on these data, α_{MIPA} can be calculated very reliably. These are shown as discrete points in Fig. 4. For comparison, the $\bar{\alpha}_{\text{MIPA}}$ curve for $x_W = 0$ given by Tikhonov regularization in Fig. 3a is reproduced in Fig. 4. There is essentially no noticeable difference between the discrete points and the continuous curve. Kell [9] tabulated α_W of pure water over a wide range of temperatures, and these are also plotted as discrete points in Fig. 4. These are compared against the $\bar{\alpha}_W$ curve for $x_W = 1$ taken from Fig. 3d. Again there is no noticeable difference between the discrete points and the continuous curve. As the two discrete sets of normal coefficients of thermal expansion for the pure components were obtained in a completely independent manner of their counterparts obtained through the partial molar volume data, the comparisons in Fig. 4 confirm not only the reliability of the $\bar{\alpha}_{\text{MIPA}}$ and $\bar{\alpha}_W$ of the pure components, but also that of all the other $\bar{\alpha}_{\text{MIPA}}$ and $\bar{\alpha}_W$ curves obtained by the same Tikhonov regularization computation.

3.3 Structure Enhancement/Destruction in Aqueous MIPA

Hepler [15] examined the second derivative of specific volume $(\partial^2 v / \partial T^2)_P$ of solutions and deduced from it whether changing the composition of a binary solution is likely to be structure promoting or destroying. The basis for this is the standard thermodynamic identity [10],

$$\left(\frac{\partial C_P}{\partial P}\right)_T = -T \left(\frac{\partial^2 v}{\partial T^2}\right)_P. \quad (7)$$

The understanding here is that, for a solution with significant structure, such as water, C_P is expected to be large compared to one with less structure. Increasing pressure P destroys the structure, i.e., $(\partial C_P / \partial P)_T$ is expected to be negative. If there is very little structure in a solution, $(\partial C_P / \partial P)_T$ is expected to be close to 0. If the structure in the solution is increased, $(\partial C_P / \partial P)_T$ is expected to become more negative. On the other hand, if the structure is reduced, $(\partial C_P / \partial P)_T$ is expected to become less negative.

In order to apply these observations to aqueous MIPA, the thermodynamic identity for $(\partial C_P / \partial P)_T$ is expressed in terms of the appropriate partial molar quantities,

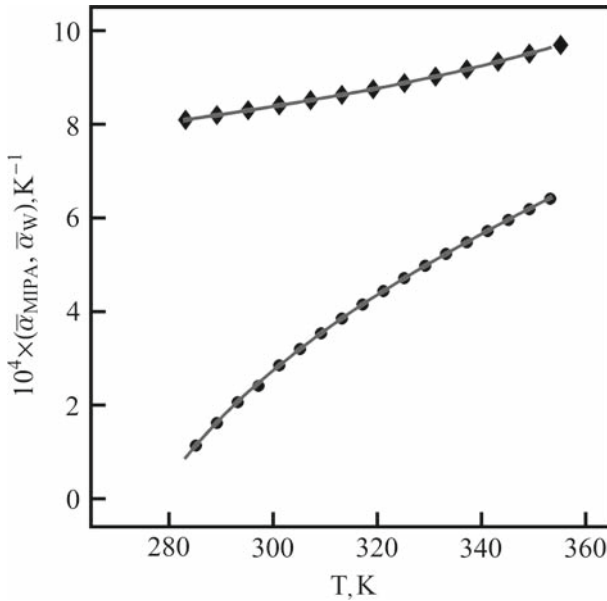


Fig. 4 Comparison of partial molar coefficients of thermal expansion with normal coefficients of thermal expansion for pure components: \blacklozenge : normal coefficient of pure MIPA [4] and \bullet : normal coefficient of pure water [9]. Curves are the partial molar coefficients from Fig. 3a for MIPA with $x_W = 0$ and from Fig. 3d for water with $x_W = 1.0$

$$\begin{aligned} \left(\frac{\partial C_P}{\partial P}\right)_T &= -T \left(\frac{\partial^2(x_W \bar{V}_W + x_{MIPA} \bar{V}_{MIPA})_{P,x_W}}{\partial T^2} \right) \\ &= -T \left[x_W \left(\frac{\partial^2 \bar{V}_W}{\partial T^2} \right)_{P,x_W} + x_{MIPA} \left(\frac{\partial^2 \bar{V}_{MIPA}}{\partial T^2} \right)_{P,x_{MIPA}} \right] \end{aligned} \quad (8)$$

According to Eq. 8, if x_{MIPA} is increased slightly, a positive $(\partial^2 \bar{V}_{MIPA} / \partial T^2)_{P,x_{MIPA}}$ will make $(\partial C_P / \partial P)_T$ more negative suggesting that this is structure promoting. Conversely, a small increase in x_{MIPA} when $(\partial^2 \bar{V}_{MIPA} / \partial T^2)_{P,x_{MIPA}}$ is negative will make $(\partial C_P / \partial P)_T$ less negative suggesting structure destruction. Similar deductions can be made with regarding to changing x_W and the sign of $(\partial^2 \bar{V}_W / \partial T^2)_{P,x_W}$.

The second derivatives $(\partial^2 \bar{V}_{MIPA} / \partial T^2)_{P,x_{MIPA}}$ given by the Tikhonov regularization computation are shown in Fig. 5a and b, and the corresponding $(\partial^2 \bar{V}_W / \partial T^2)_{P,x_W}$ are shown in Fig. 5c. The $(\partial^2 \bar{V}_W / \partial T^2)_{P,x_W}$ curves in Fig. 5c do not exhibit any clear pattern as T is increased. With the limited non-isothermal data available, it is doubtful that a detailed analysis of their trend can be justified. But it is also clear from Fig. 5c that all the $(\partial^2 \bar{V}_W / \partial T^2)_{P,x_W}$ are essentially positive. Hence, water can be regarded as structure promoting. Similarly, $(\partial^2 \bar{V}_{MIPA} / \partial T^2)_{P,x_{MIPA}}$ for $0 \leq x_W \leq 0.5$ in Fig. 5a also shows no discernable trends, but they are all positive. The $(\partial^2 \bar{V}_{MIPA} / \partial T^2)_{P,x_{MIPA}}$ for $0.6 \leq x_W \leq 1.0$ in Fig. 5b are more regular, and they again remain positive except

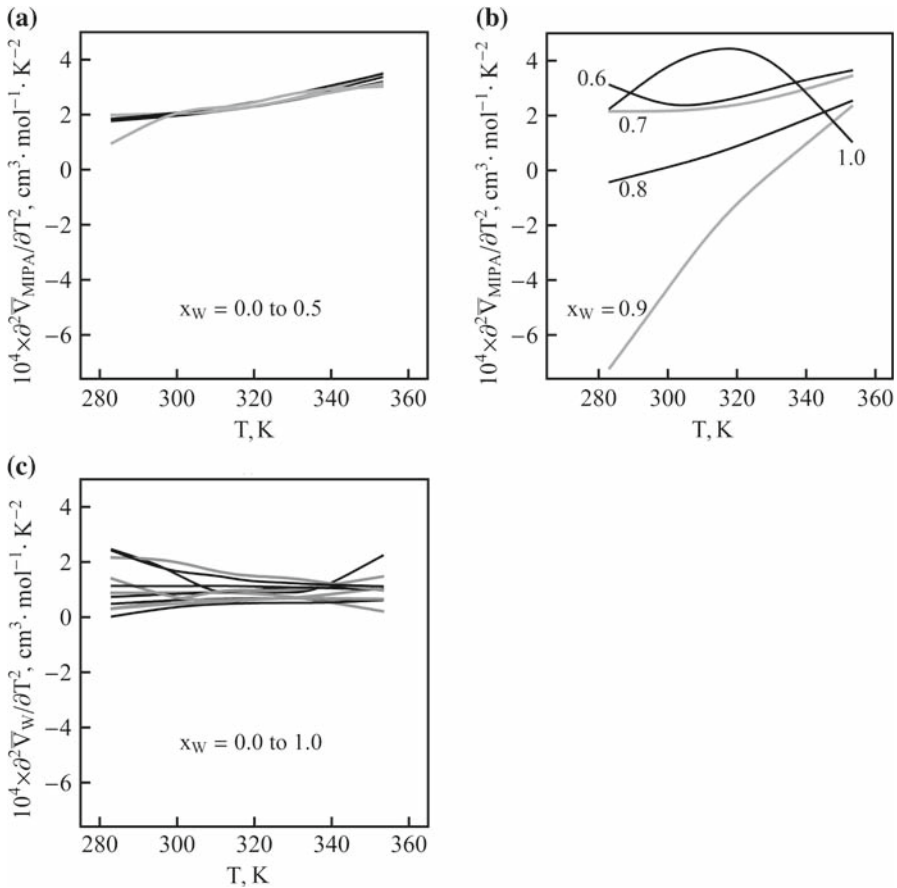


Fig. 5 The second derivatives of partial molar volumes with respect to temperature: (a), (b) MIPA and (c) water. For curves that are spaced out, the value of x_W is shown beside each of the curves

in the neighborhood of $x_W = 0.9$. Thus, in general, MIPA also appears to be structure promoting. At $x_W = 0.9$, $(\partial^2 \bar{V}_{\text{MIPA}} / \partial T^2)_{P, x_{\text{MIPA}}}$ is negative for $T < 335$ K (approx.) suggesting that the addition of MIPA to water under this condition is structure destroying. But this ceases to be so with further addition of MIPA. This changeover from structure destroying to structure promoting occurs between $x_W = 0.9$ and $x_W = 1$. However, without specific knowledge of the nature of the structure or structures in aqueous MIPA solutions under different temperatures and concentrations, this brief discussion of structure, promoting or destroying, should be treated as tentative or even speculative.

Figure 2 shows that all the \bar{V}_{MIPA} and \bar{V}_W , at constant composition, are relatively linear in T . Consequently, the second derivatives $(\partial^2 \bar{V}_{\text{MIPA}} / \partial T^2)_{P, x_{\text{MIPA}}}$ and $(\partial^2 \bar{V}_W / \partial T^2)_{P, x_W}$ are expected to be close to 0. According to Tikhonov regularization, they are indeed very small, only of the order of $10^{-4} \text{ cm}^3 \cdot \text{mol}^{-1} \cdot \text{K}^{-2}$. As the computation of \bar{V}_{MIPA} and \bar{V}_W requires the first derivative of the experimentally

measured specific volume $v(x_W)$, their second derivatives with respect to T are therefore effectively the third derivative of $v(x_W)$ —once with respect to x_W and twice with respect to T . Evaluation of the higher derivatives of experimental data poses considerable computational problems [7]. It is not surprising that Mokraoui et al. [4] reported difficulties in obtaining $(\partial^2 \bar{V}_{\text{MIPA}} / \partial T^2)_{P, x_{\text{MIPA}}}$ and $(\partial^2 \bar{V}_W / \partial T^2)_{P, x_W}$. The second derivatives in Fig. 5 demonstrate the advantages of Tikhonov regularization over the conventional curve fitting technique. The reliability of these second derivatives can be further improved if the experimental $\rho(x_W)$ or $v(x_W)$ data are available over a wider temperature range and possibly at a smaller temperature interval. The former is physically attainable, but the latter may raise a number of practical issues.

4 Conclusion

Tikhonov regularization provides an efficient way of computing the various derivatives of the molar volume data of aqueous MIPA. These derivatives allow the partial molar volumes and the partial molar coefficients of thermal expansion to be evaluated reliably. The change in the sign of the second derivatives of the partial molar volumes with respect to temperature provides a means of investigating, albeit with some uncertainty, the structure forming and destroying role of MIPA and water at different temperatures and for different compositions.

References

1. M.M. Sharma, P.V. Danckwerts, *Chem. Eng. Sci.* **18**, 735 (1963)
2. H. Hikita, H. Ishikawa, T. Murakami, T. Ishii, *J. Chem. Eng. Jpn* **14**, 411 (1981)
3. F. Camacho, S. Sánchez, R. Pacheco, *Ind. Eng. Chem. Res.* **36**, 4358 (1997)
4. S. Mokraoui, A. Valtz, C. Coquelet, D. Richon, *Thermochem. Acta* **440**, 122 (2006)
5. S. Mokraoui, A. Valtz, C. Coquelet, D. Richon, *Thermochem. Acta* **471**, 106 (2008)
6. M. Mundhwa, A. Henni, *J. Chem. Eng. Data* **52**, 491 (2007)
7. H.W. Engl, M. Hanke, A. Neubauer, *Regularization of Inverse Problems* (Kluwer, Dordrecht, 2000)
8. A.S. Lubansky, Y.L. Yeow, Y.K. Leong, S.R. Wickramasinghe, B. Han, *AIChE J.* **52**, 323 (2006)
9. G.S. Kell, *J. Chem. Eng. Data* **12**, 66 (1967)
10. S.I. Sandler, *Chemical, Biochemical and Engineering Thermodynamics*, 4th edn. (Wiley, New York, 2006)
11. Y.L. Yeow, Y.-K. Leong, *J. Chem. Thermodyn.* **39**, 1675 (2007)
12. Y.L. Yeow, Y.-K. Leong, *J. Solution Chem.* **36**, 1047 (2007)
13. J.G. Burkill, *A First Course in Mathematical Analysis* (CUP, Cambridge, 1978)
14. G. Wahba, *Spline Models for Observational Data* (SIAM, Philadelphia, 1990)
15. L.G. Hepler, *Can. J. Chem.* **47**, 4613 (1969)